INSTITUT DE FRANCE
Académie des sciences

# Comptes Rendus

# Physique

Frederic Teubert and Pippa Wells

**$W^{\pm}$ and $Z^{0}$ boson physics**

Volume 21, issue 1 (2020), p. 9-22.

<https://doi.org/10.5802/crphys.7>

**Part of the Thematic Issue:** A perspective of High Energy Physics from precision measurements

**Guest editors:** Stéphane Monteil (Clermont Université, CNRS/IN2P3, Clermont-Ferrand) and Marie-Hélène Schune (Université Paris-Saclay, CNRS/IN2P3, Orsay)



*Les* Comptes Rendus. Physique *sont membres du Centre Mersenne pour l'édition scientifique ouverte*
www.centre-mersenne.org

*Comptes Rendus*
*Physique*
**2020**, 21, nº 1, p. 9-22
https://doi.org/10.5802/crphys.7

A perspective of High Energy Physics from precision measurements
*La physique des Hautes Energies du point de vue des mesures de précision*

# $W^{\pm}$ and $Z^0$ boson physics

## *La physique des bosons $W^{\pm}$ et $Z^0$*

**Frederic Teubert**[*, a] **and Pippa Wells**[a]

[a] European Organization for Nuclear Research (CERN), Geneva, Switzerland.
*E-mails:* frederic.teubert@cern.ch (F. Teubert), pippa.wells@cern.ch (P. Wells).

**Abstract.** Precision measurements of the weak bosons ($Z^0$ and $W^{\pm}$) at $e^+e^-$ and hadron colliders have allowed the Standard Model to be tested as a quantum field theory, requiring the inclusion of higher order quantum loop corrections. The agreement of these measurements with the Standard Model puts strong constrains on New Physics scenarios. To achieve such precision, a close collaboration between experimenters and theorists, as well as between experimenters in different collaborations was pioneered in the 90s. A superb control of the experimental systematic uncertainties as well as an unprecedented level of precision on the collider beam energy and intensity was required in many of these measurements. New accelerators are proposed in the future that could improve these tests of the Standard Model even further.

**Résumé.** Les mesures de précision effectuées sur les bosons $W^{\pm}$ et $Z^0$ aux collisionneurs $e^+e^-$ et hadroniques ont permis de tester le Modèle Standard en tant que théorie quantique des champs, c'est-à-dire incluant des corrections quantiques d'ordre élevé. L'accord entre ces mesures et le Modèle Standard contraint fortement les scenarii de nouvelle physique. Des collaborations étroites entre expérimentateurs et théoriciens ainsi qu'entre expérimentateurs des différentes expériences, telles que celles engagées dans les années 1990, sont indispensables pour atteindre une grande precision. Un excellent contrôle des incertitudes systématiques expérimentales ainsi qu'une détermination de l'énergie des faisceaux et de leur intensité avec un niveau de précision qui n'avait encore jamais été atteint ont été indispensables pour un grand nombre de ces mesures. De futurs accélérateurs sont actuellement proposés afin d'accroître encore la précision de ces tests du Modèle Standard.

**Keywords.** Large hadron collider, $Z^0$, $W^{\pm}$.

**Mots-clés.** Grand collisionneur de hadrons, $Z^0$, $W^{\pm}$.

## 1. Historical introduction

By the end of the 19th century several types of radioactivity had been discovered in heavy elements like Uranium, Thorium, Polonium and Radium. In 1899, Ernest Rutherford had separated radioactive emissions into two types: $\alpha$ and $\beta$-decays based on the penetration of objects and

* Corresponding author.

the ability to cause ionisation. While $\alpha$-rays could be stopped by thin sheets of aluminium, $\beta$-rays could penetrate several millimetres of aluminum. Later a third type of even more penetrating radiation, $\gamma$-rays, was identified. In 1900 Becquerel had measured the mass-to-charge ratio ($m/e$) for $\beta$ particles and found the same as for Thomson's electron, therefore concluding that $\beta$-rays were in fact electrons. The energy distribution of these $\beta$-rays was not a narrow peak (like for the other types of radiation) but a continuous distribution that forced Pauli in 1930 to propose the existence of a new extremely light neutral particle, the neutrino, in order to preserve the conservation of energy in the process.

To explain $\beta$-decays a new type of nuclear interaction was needed (Weak Interactions). Enrico Fermi came up in 1933 with a useful theory [1, 2] to explain the neutron $\beta$-decay by direct coupling of a neutron with an electron, a neutrino (later determined to be an antineutrino) and a proton. The Fermi interaction was the precursor to the theory for the weak interaction where the interaction is mediated by a virtual $W^{\pm}$ boson, of which Fermi theory is the low-energy effective field theory. In fact, following the success of the gauge field theory for electromagnetic interactions (QED) in the 1950s, Glashow, Weinberg and Salam (GWS) [3–5] efforts to replace Fermi's effective theory culminated around 1968 with a unified theory of electromagnetism and weak interactions. Their electroweak (EW) theory postulated not only the $W^{\pm}$ boson to explain $\beta$ decays, but also a new $Z^0$ boson that had never been observed and would induce neutral weak current interactions.

### 1.1. *Neutral current interactions in neutrino scattering experiments*

In 1973 neutral current interactions were indeed observed [6, 7] as predicted by theory. The huge "Gargamelle" bubble chamber made use of a neutrino beam produced from $\pi \to \mu\nu_\mu$ and $K \to \mu\nu_\mu$ decays, produced by a proton beam from the CERN Proton-Synchrotron (PS) accelerator. The Gargamelle collaboration discovered both leptonic neutral currents (events involving the interaction of an incoming neutrino with an electron), and hadronic neutral currents (events when an incoming neutrino is scattered from a nucleon). This experimental confirmation was crucial in establishing the GWS theory of electroweak interactions which is one of the pillars of the Standard Model (SM) today.

### 1.2. *Discovery of $Z^0$ and $W^{\pm}$ at CERN*

The discovery of the $W^{\pm}$ and $Z^0$ bosons themselves had to wait for the construction of a particle accelerator powerful enough to produce them. Within the framework of the SM, the observation of neutral currents in neutrino induced reactions allowed the first quantitative prediction for the mass of the weak bosons in the range 60 to 80 GeV for the $W^{\pm}$ and 75 to 92 GeV for the $Z^0$ bosons. In 1976 Rubbia, Cline and McIntyre proposed [8] the transformation of the new CERN Super-Proton-Synchrotron (SPS) accelerator into a $p\overline{p}$ collider as a quick and relatively cheap way to achieve collisions above threshold for $W^{\pm}$ and $Z^0$ production. By the end of 1982, the $p\overline{p}$ collision rate was high enough to permit the observation of $W \to e\nu_e$ decays [9, 10]. In a subsequent run during the spring of 1983, the decays $Z^0 \to e^+e^-$ and $Z^0 \to \mu^+\mu^-$ were also observed [11, 12], vindicating the GWS theory of Electroweak interactions. Figure 1 shows the invariant mass distribution of events recorded by the UA1 and UA2 Collaborations enabling the discovery of the $Z^0$ boson.

## 2. Theory context

In the context of the SM, any EW process can be computed at tree level from $\alpha$ (the fine structure constant measured at values of $q^2$ close to zero), $m_W$ (the $W^{\pm}$-boson mass), $m_Z$ (the

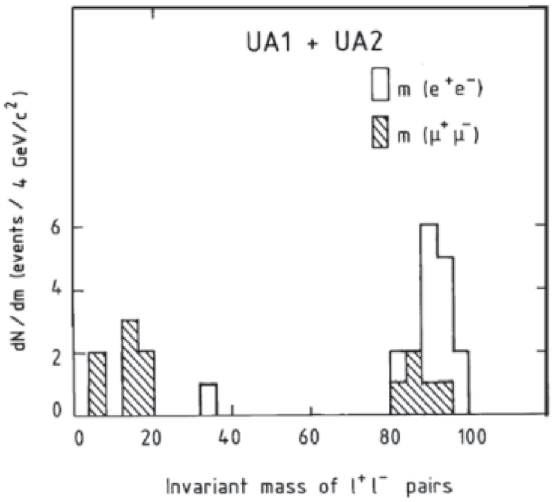


**Figure 1.** Invariant mass distribution of dilepton events from UA1 and UA2 experiments. A clear peak is visible at a mass of about 95 GeV (taken from http://www.nobelprize.org/).

$Z^0$-boson mass), and $V_{jk}$ (the Cabbibo–Kobayashi–Maskawa flavour-mixing matrix elements). When higher order corrections are included, any observable can be predicted in the "on-shell" renormalisation scheme as a function of:

$$O_i = f_i(\alpha, \alpha_s, m_W, m_Z, m_H, m_f, V_{jk})$$

and contrary to what happens with "exact gauge symmetry theories", like QED or QCD, the effects of heavy particles in the EW interactions do not decouple. Therefore, the SM predictions of the EW interactions at $q^2 \sim {m_Z}^2$ depend on the top quark mass ($(m_t^2 - m_b^2)/m_Z^2$) and to a lesser extent on the Higgs boson mass ($\log(m_H^2/m_Z^2)$), or to any kind of "heavy new physics".

The $W^{\pm}$ mass is one of the input parameters in the "on-shell" renormalisation scheme. As discussed later, $m_W$ is measured with a precision of about 0.015%, although the usual procedure is to take $G_\mu$ (the Fermi constant measured in the muon decay known with an even better precision of about 0.0009%) to predict $m_W$ as a function of the rest of the input parameters. The less well known input parameters are $\alpha_s$, $m_t$ and $m_H$, measured today with a precision of about 1%, 0.2% and 0.1% respectively. The value of $\alpha^{-1}(m_Z^2)$ is only known with a relative precision of about 0.01%, even though its value at $q^2 \sim 0$ is known with an amazing relative precision of $4 \times 10^{-9}$ due to the uncertainties in the calculation of the running of $\alpha$. In fact, given the accuracy already achieved and described in the next sections, an effort would be needed to improve the accuracy of the input parameters, and in particular $\alpha({m_Z}^2)$, if the precision of future measurements is not to be jeopardised.

From the point of view of EW radiative corrections we can divide the experimental measurements into four different groups: the $Z^0$ total and partial widths ($\Gamma_Z$), the partial width into $b$-quarks ($R_b$), the $Z^0$ asymmetries ($\sin^2\theta^{\text{lept}}_{\text{eff}}$) and the $W^{\pm}$ mass ($m_W$). For instance, the $Z^0$ leptonic width is mostly sensitive to isospin-breaking loop corrections ($\Delta\rho$), the asymmetries are specially sensitive to radiative corrections to the $Z^0$ self-energy ($\Delta\kappa$ ), and $R_b$ is mostly sensitive to vertex corrections ($\epsilon_b$) in the decay $Z^0 \to b\bar{b}$. One more parameter, $\Delta r$, is necessary to describe the radiative corrections to the relation between $G_\mu$ and $m_W$, and in fact it is the measured $\Delta r$ the most significant evidence for pure EW radiative corrections in agreement with the GWS theory.

### 2.1. *Definition of pseudo-observables at the $Z^0$ pole*

The shape of the resonance is completely characterised by three parameters: the position of the peak ($m_Z$), the width ($\Gamma_Z$) and the height ($\sigma^0_{f\bar{f}}$) of the resonance:

$$\sigma^0_{f\bar{f}} = \frac{12\pi}{m_Z^2}\frac{\Gamma_e\Gamma_f}{\Gamma_Z^2}.$$

The good capabilities of the LEP and SLC detectors to identify lepton flavours allows a measurement of the ratio of the different lepton species with respect to the hadronic cross-section, $R_\ell = \Gamma_h/\Gamma_\ell$. The large mass and long lifetime of the $b$ and $c$ quarks provides a way to perform flavour tagging. This allows for precise measurements of the partial widths of the decays $Z^0 \to c\bar{c}$ and $Z^0 \to b\bar{b}$. It is useful to normalise the partial width to $\Gamma_h$ by measuring the partial decay fractions with respect to all hadronic decays:

$$\mathrm{R}_c \equiv \frac{\Gamma_c}{\Gamma_h}, \quad \mathrm{R}_b \equiv \frac{\Gamma_b}{\Gamma_h}.$$

With this definition most of the radiative corrections appear both in the numerator and denominator and thus cancel out, with the important exception of the vertex corrections in the $Z^0 b\bar{b}$ vertex. This is the only relevant correction to $\mathrm{R}_b$, and within the SM basically depends on a single parameter, the mass of the top quark. The partial decay fractions of the $Z^0$ to other quark flavours, like $\mathrm{R}_c$, are only weakly dependent on $m_t$; the residual weak dependence is indeed due to the presence of $\Gamma_b$ in the denominator. The SM predicts $\mathrm{R}_c = 0.172$, valid over a wide range of the input parameters.

Parity violation in the weak neutral current is caused by the difference of couplings of the $Z^0$ to right-handed and left-handed fermions. If we define $A_f$ as

$$A_f \equiv \frac{2\left(\frac{g_V^f}{g_A^f}\right)}{1+\left(\frac{g_V^f}{g_A^f}\right)^2},$$

where $g^f_{V(A)}$ denotes the vector (axial-vector) coupling constants of the $Z^0$ and the corresponding fermion, one can write all the $Z^0$ asymmetries in terms of $A_f$.

Each process $e^+e^- \to Z \to f\bar{f}$ can be characterised by the direction and the helicity of the emitted fermion ($f$). Calling forward the hemisphere into which the electron beam is pointing, the events can be subdivided into four categories: FR, BR, FL and BL, corresponding to right-handed (R) or left-handed (L) fermions emitted in the forward (F) or backward (B) direction. Then, one can write three $Z^0$ asymmetries as:

$$\begin{aligned}
A_{\mathrm{pol}} &\equiv \frac{\sigma_{\mathrm{FR}} + \sigma_{\mathrm{BR}} - \sigma_{\mathrm{FL}} - \sigma_{\mathrm{BL}}}{\sigma_{\mathrm{FR}} + \sigma_{\mathrm{BR}} + \sigma_{\mathrm{FL}} + \sigma_{\mathrm{BL}}} = -A_f, \\
A^{\mathrm{FB}}_{\mathrm{pol}} &\equiv \frac{\sigma_{\mathrm{FR}} + \sigma_{\mathrm{BL}} - \sigma_{\mathrm{BR}} - \sigma_{\mathrm{FL}}}{\sigma_{\mathrm{FR}} + \sigma_{\mathrm{BR}} + \sigma_{\mathrm{FL}} + \sigma_{\mathrm{BL}}} = -\frac{3}{4}A_e, \\
A_{\mathrm{FB}} &\equiv \frac{\sigma_{\mathrm{FR}} + \sigma_{\mathrm{FL}} - \sigma_{\mathrm{BR}} - \sigma_{\mathrm{BL}}}{\sigma_{\mathrm{FR}} + \sigma_{\mathrm{BR}} + \sigma_{\mathrm{FL}} + \sigma_{\mathrm{BL}}} = \frac{3}{4}A_eA_f
\end{aligned}$$

and in case the initial state is polarised with some degree of polarisation ($P$), one can define:

$$\begin{aligned}
A_{\mathrm{LR}} &\equiv \frac{1}{P}\frac{\sigma_{\mathrm{Fl}} + \sigma_{\mathrm{Bl}} - \sigma_{\mathrm{Fr}} - \sigma_{\mathrm{Br}}}{\sigma_{\mathrm{Fr}} + \sigma_{\mathrm{Br}} + \sigma_{\mathrm{Fl}} + \sigma_{\mathrm{Bl}}} = A_e, \\
A^{\mathrm{pol}}_{\mathrm{FB}} &\equiv -\frac{1}{P}\frac{\sigma_{\mathrm{Fr}} + \sigma_{\mathrm{Bl}} - \sigma_{\mathrm{Fl}} - \sigma_{\mathrm{Br}}}{\sigma_{\mathrm{Fr}} + \sigma_{\mathrm{Br}} + \sigma_{\mathrm{Fl}} + \sigma_{\mathrm{Bl}}} = \frac{3}{4}A_f
\end{aligned}$$

where r(l) denotes the right(left)-handed initial state polarisation. Assuming lepton universality, all these observables depend only on the ratio between the vector and axial-vector couplings between the $Z^0$ boson and the leptons. It is conventional to define the effective mixing angle $\sin^2\theta^{\text{lept}}_{\text{eff}}$ as

$$\sin^2\theta^{\text{lept}}_{\text{eff}} \equiv \frac{1}{4}\left(1 - \frac{g^l_V}{g^l_A}\right)$$

and to convert all the asymmetry measurements into a single parameter $\sin^2\theta^{\text{lept}}_{\text{eff}}$.

## 3. Precision measurements at $e^+e^-$ colliders

### 3.1. *Precise energy determination at LEP*

Knowledge of the LEP beam energy is fundamental to the determination of the $Z^0$ mass and width [13], and the $W^\pm$ mass [14], and gradual unravelling of unexpected systematic effects took years in order to achieve the final precision.

Of historical interest, protons circulated around the ring for the first time in 1989, long before the advent of the LHC. Their speed at injection energy, 20 GeV, was inferred by comparing the radio-frequency needed to maintain protons and electrons on the LEP central orbit (through the centre of the focussing quadrupoles). This was extrapolated to 45 GeV using magnetic measurements to give a 20 MeV uncertainty on the $Z^0$ mass; the beam energy is proportional to the total magnetic field seen by the beam, $\oint B\cdot \mathrm{d}\ell$. However, the beam energy can be determined much more precisely with the technique of resonant depolarisation. The electron spin tends to align with the bending field due to synchrotron radiation, and significant polarisation can build up if the beam orbit is sufficiently smooth. The spins precess, with the number of precessions per orbit, $\nu_s$, given by:

$$\nu_s = \frac{g_e - 2}{2}\frac{e}{2\pi m_e}\oint B\cdot \mathrm{d}\ell = \frac{g_e - 2}{2}\frac{E_{\text{beam}}}{m_e}. \tag{1}$$

The polarisation is monitored, as the frequency of a fast sweeping horizontal magnetic field is varied. This depolarises the beam when the external field frequency matches $\nu_s$. The instantaneous precision on the beam energy is $\mathcal{O}(100)$ keV, but the technique can not be used when the beams are in collision. Instead the beam energy could be measured at the ends of fills. However, the beam energy was found to vary with time. In Figure 2, the results of several long term experiments to monitor the beam energy with resonant depolarisation were understood to be due to earth tides. The length of the beam orbit is fixed by the radio frequency (RF) accelerating cavities. The bulge of the earth due to tides changes the length of the tunnel by about 1 mm in 27 km, so the magnets move with respect to the beam. The extra contribution from the quadrupoles changes the beam energy with an amplitude of about 10 MeV.

In 1995, two NMR probes were installed in LEP dipoles to monitor the bending field on opposite sides of the ring. There was noise related to some unknown activity, with a quiet period over night, resulting in a general trend for the energy to increase during a fill. The beam energy measurement from the end of a fill was giving a bias of typically 5 MeV. This was eventually understood as being due to vagabond currents from the French high speed trains (TGV). A strong correlation was observed as a function of time between the current measured on the rail lines, the voltage on the LEP beam pipe, and the field measured by the NMRs. The return current from the trains from the nearest point labelled "Zimeysa" in Figure 2 flowed back to the power station in two directions round the ring, and then via a local river. A model to describe this average behaviour was derived and restrospectively applied to all the previous years' data [13]. This model took into account other effects including magnet temperatures, and interaction point dependent effects.

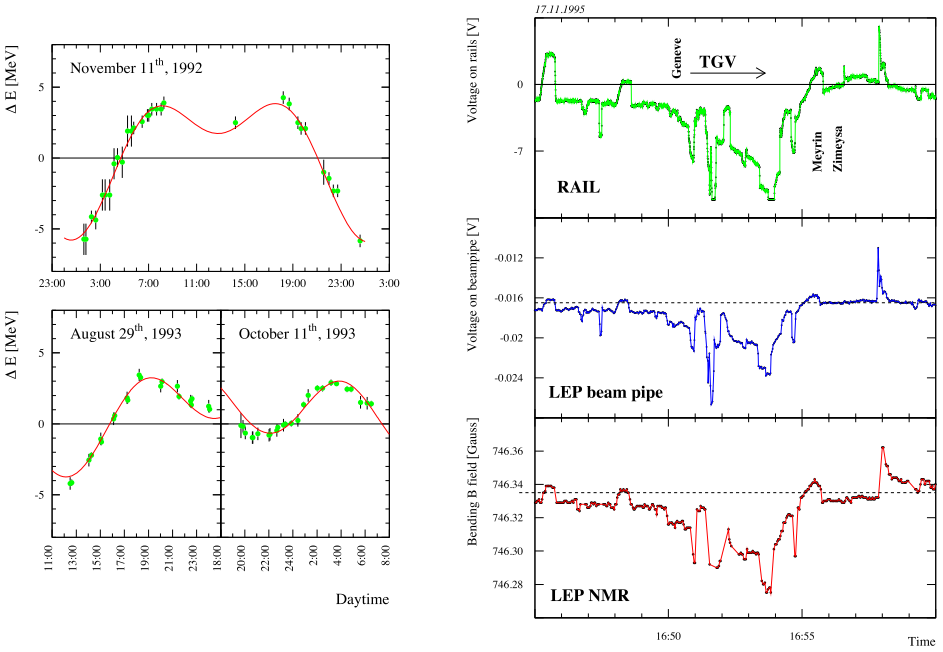


**Figure 2.** (left) Tides and polarisation measurement. Results from repeated beam energy measurements by resonant depolarisation (points), compared to the prediction of the energy taking into account earth tides (curves). (right) Simultaneous measurements of the current on the rail lines, the voltage on the LEP beam pipe, and the dipole magnetic field as a TGV leaves Geneva.

The collision energy was expected to be the same at all four interaction points, but already with the 1991 data, the results showed a trend for OPAL and L3 to have a lower value for the $Z^0$ mass than ALEPH and DELPHI. The discrepancy was traced to the positioning of the RF cavities. They were aligned to the wrong frequency, so that in practice the collision energy was higher in OPAL and L3. The exact configuration of the RF cavities was even more important as the beam energy increased during LEP2. In addition, the beam polarisation decreased as the beam energy increased, so for the measurement of the $W^{\pm}$ mass, magnetic extrapolation was again needed from resonant depolarisation measurements spanning up to 65 GeV and the full beam energy [14]. Additional NMR probes, two per octant, were installed, which also helped to validate the LEP1 beam energy model. A new spectrometer was also installed; a standard LEP dipole magnet was replaced by a shorter, precisely-mapped steel dipole magnet. Beam pickup monitors either side of this new dipole allowed a precise measurement of the bending angle to yield an independent measurement of the beam energy which was again cross-calibrated at lower energy with resonant depolarisation.

As a result of these very detailed studies and many careful cross checks, the final uncertainty due to the centre-of-mass energy was 1.7 MeV for the $Z^0$ mass, out of a total uncertainty of 2.1 MeV. The uncertainty increased to 10 MeV for the $W^{\pm}$ mass measurement, but this was still a relatively small component of the LEP combined 33 MeV uncertainty.

### 3.2. *Polarisation at SLC*

The SLC was the first $e^+e^-$ linear collider. The era of high precision measurements at SLC started in 1992 with the first longitudinally polarised beams. The polarisation was achieved by shining

circularly polarised laser light on a gallium arsenide photo-cathode at the electron source. At that time, the electron polarisation was only $P \sim 22\%$. Shortly thereafter, improvements in the photocathodes allowed to increase the polarisation significantly, close to $P \sim 75\%$. Much work was invested in the SLC machine to maintain the electron polarisation at a very high value throughout the production, damping, acceleration and transfer through the arcs. The polarised beam physics programme at the SLC required additional instrumentation beyond the main SLD detector, most notably, precision polarimetry. A Compton-scattering polarimeter installed near the beam interaction point reached an ultimate precision of $\Delta P \sim 0.5\%$ which ensured that polarimetry systematics were never the leading contribution to the uncertainties.

### 3.3. *Detectors at LEP/SLC*

The designs of the LEP and SLC detectors are quite similar, although the details vary significantly among them. Starting radially from the interaction point, there is first a vertex detector, followed by a gas drift chamber to measure the parameters of charged tracks. Surrounding the tracking system is a calorimeter system, usually divided into electromagnetic and hadronic sections. Finally, an outer tracking system designed to measure the parameters of penetrating particles (muons) completes the system. The central part of the detector (at least the tracking chamber) is immersed in a solenoidal magnetic field to allow the measurement of the momentum of charged particles. In addition, particle identification systems may be installed, including $\mathrm{d}E/\mathrm{d}x$ ionisation loss measurements in the central chamber, time-of-flight, and ring-imaging Cherenkov detectors.

Special detectors extending to polar angles of ~25 mrad with respect to the beam axis detect small-angle Bhabha scattering events. The rate of these events was used for the luminosity determinations, as the small-angle Bhabha process is due almost entirely to QED, and the cross-section can be calculated precisely. All the LEP experiments replaced their first-generation luminosity detectors, which had systematic uncertainties at the percent level, with high-precision devices capable of pushing systematic uncertainties on the acceptance of small-angle Bhabha scattering events below one per-mille.

As a consequence of the improvements to the detectors and also in the understanding of the beam energy at LEP1, and the production of high beam polarisation at SLC, statistical and systematic uncertainties are much smaller for the later years of data taking, which hence dominate the precision achieved on the $Z^0$ parameters. All five detectors had almost complete solid angle coverage; the only holes being at polar angles below the coverage of the luminosity detectors.

### 3.4. *LEP/SLC combination and results*

The LEP electroweak working group was established in the early 1990s, including physicists from all four experiments to combine the cross-section and forward-backward asymmetry measurements at each energy point. The level of sophistication of the combinations was refined over the years as the statistical and systematic uncertainties improved. Correlations between experiments were carefully evaluated, including common effects coming from the LEP beam energy measurement, theoretical modelling of $Z^0$ decays and backgrounds, and Monte Carlo treatment of fragmentation and hadronisation.

In some areas, such as $Z^0$ decays to heavy-flavour quarks, this took detailed negotiations to agree on common treatments of systematic effects, and by 1994, results from the SLD heavy-flavour group were also included in a coherent way. While for the main lineshape and lepton asymmetry measurements, each experiment measured the same set of parameters, the situation was more complicated for heavy-flavour electroweak results. Different experiments used different tagging methods; some analyses made combined fits which included semileptonic branching

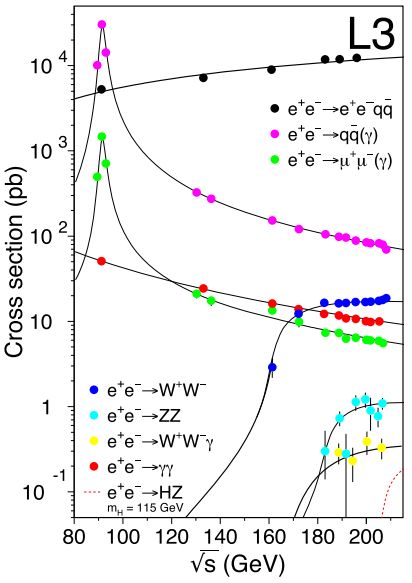


**Figure 3.** Measurements of various cross-sections in $e^+e^-$ collisions. This example is from the L3 collaboration, and indicates the precision around the $Z^0$ peak, and as $e^+e^- \to W^\pm W^\pm$ is accessible at higher centre-of-mass energies.

ratios and $B^0$ mixing parameters; the measurements could have an explicit dependence on other parameters such as the partial widths to $b$- and $c$-quarks, introducing additional correlations.

The results from 18 million $Z^0$ decays from the four LEP experiments, ALEPH, DELPHI, L3 and OPAL, and from the SLD experiment at SLC, provide numerous measurements of $Z^0$ boson properties, from inclusive hadron production, and from pair-production of charged leptons and heavy quarks. The production cross-sections and asymmetries as a function of centre of mass energies yield the combined results [15]

$$\begin{aligned} m_Z &= 91.1875 \pm 0.0021 \text{ GeV}/c^2, \\ \Gamma_Z &= 2.4952 \pm 0.0023 \text{ GeV}, \\ \rho_\ell &= 1.0050 \pm 0.0010, \\ \sin^2\theta^{\text{lept}}_{\text{eff}} &= 0.23153 \pm 0.00016, \\ N_\nu &= 2.9840 \pm 0082. \end{aligned}$$

The sensitive test of lepton universality in $Z^0$ decays is demonstrated in Figure 4, comparing the combined left and right-handed couplings for the three types of charged lepton. The full set of combined measurements is listed in Figure 5, where the results are also compared to a global fit including other measurements at the time of the final LEP 1 publication [15].

The LEP measurements of the $W^\pm$-boson mass [16] are shown in Figure 6 where they are also compared with measurements from hadron colliders, which are discussed in the next section.

## 4. Precision measurements at hadron colliders

### 4.1. $W^\pm$ *mass measurements*

At hadron colliders, precision measurements of $W^\pm$ and $Z^0$ properties are limited to leptonic final states with electrons or muons. The main parameter of interest is the $W^\pm$ mass. Samples of $Z^0 \to$

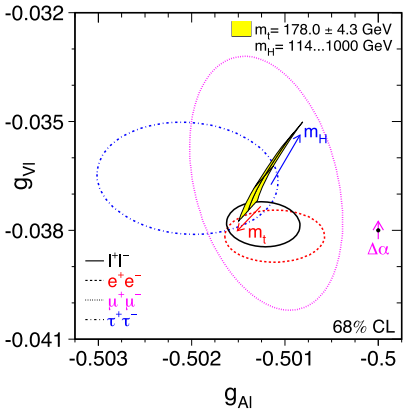


**Figure 4.** Comparison of the effective vector and axial-vector coupling constants for leptons. The shaded region shows the SM prediction with $m_t = 178.0 \pm 4.3$ GeV and $m_H = 300^{+700}_{-186}$ GeV.

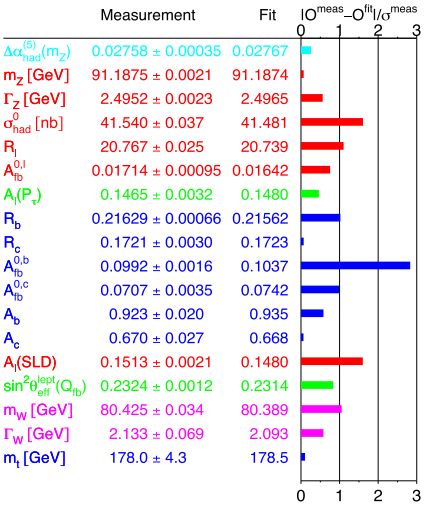


**Figure 5.** Comparison of measurements with the SM prediction from the best fit. Also shown is the pull of each measurement, defined as the difference between the measurement an expectation in units of the measurement uncertainty.

$e^+e^-$ or $\mu^+\mu^-$ are typically used to calibrate the energy or momentum response of the detector, normalising to the LEP measurement. $Z^0$ boson samples are also of use to control systematic uncertainties in the prediction of the $W^\pm$ transverse momentum spectrum. Production of $W^\pm$ and $Z^0$ bosons is dominated by quark-antiquark annihilation.

The $W^\pm$ mass is determined from fits to the distributions of the transverse momentum of the charged lepton, $p_{\mathrm{T}}^{\ell}$, the neutrino, $p_{\mathrm{T}}^{\nu}$, and of the transverse mass, $m_{\mathrm{T}}$. The neutrino transverse momentum is taken to be the missing transverse momentum, $p_{\mathrm{T}}^{\mathrm{miss}}$, estimated from the negative vector sum of the transverse momenta of visible particles. The transverse mass is defined by $m_{\mathrm{T}}^2 = 2p_{\mathrm{T}}^{\ell}p_{\mathrm{T}}^{\mathrm{miss}}(1-\cos\Delta\phi)$, where $\Delta\phi$ the azimuthal opening angle between the charged lepton and missing transverse momentum. The kinematic distributions depend on detector effects, and also the modelling of the $W^\pm$ transverse momentum and parton distribution fuctions (PDFs).

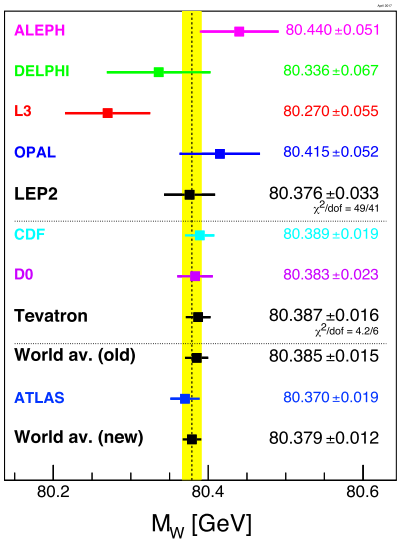


**Figure 6.** The latest world average $W^{\pm}$ mass from the Tevatron electroweak working group, and an update by the PDG including the new ATLAS result.

Valence (anti)quarks dominate at the Tevatron, while in higher-energy proton-proton collisions at the LHC, sea-quarks play a much more important role.

The Tevatron combined result is dominated by the most recent CDF and D0 measurements [17]. The CDF result uses $W \to \mu\nu$ and $W \to e\nu$ events in 2.2 fb$^{-1}$ recorded between 2002 and 2007. The momentum scale from $J/\psi$ and $\Upsilon$ decays to muon pairs yields a $Z^0$ mass consistent with the LEP average, so this is used as an additional constraint. The electromagnetic energy scale is determined from a fit to the $E/p$ distribution for electrons in $W^{\pm}$ and $Z^0$ decays. The $Z^0$ mass is again used as a consistency check and a constraint. The CDF measurement is obtained from a combination of all six observables, $p_{\mathrm{T}}^{\ell}$, $p_{\mathrm{T}}^{\nu}$ and $m_{\mathrm{T}}$ for muons and for electrons. The most precise D0 measurement is from 4.3 fb$^{-1}$ recorded between 2006 and 2009, and only uses electrons. The energy scale is calibrated from $Z^0$ decays. The result combines the $p_{\mathrm{T}}^{e}$ and $m_{\mathrm{T}}$ distributions, and an earlier measurement using 1.0 fb$^{-1}$ recorded in 2002 to 2006.

The overall Tevatron combined precision is 16 MeV [17], compared to the combined LEP precision of 33 MeV, and leading to a world average $W^{\pm}$ mass from 2013 of $80.385 \pm 0.015$ GeV. This is displayed in Figure 6 [18].

ATLAS published their first $W^{\pm}$ mass measurement using the 7 TeV dataset recorded in 2011 [19]. The analysis uses $W \to e\nu$ and $W \to \mu\nu$ events, making template fits to the lepton $p_{\mathrm{T}}$ or the transverse mass, $m_{\mathrm{T}}$, of the $\ell\nu$ system. A sample of $Z \to \ell\ell$ events is also used for calibration; calibration of the leptons and of the hadronic recoil to the $W^{\pm}$ boson is the biggest experimental challenge in this measurement. The multijet background is evaluated from fits in bins of lepton isolation, which are then extrapolated to isolated leptons in the $W^{\pm}$ sample.

With the experimental uncertainties under control, physics modelling uncertainties dominate. These are also controlled by comparison to $W^{\pm}$ or $Z$ data in order to rule out large model variations, for example of the vector boson $p_{\mathrm{T}}$ spectrum. Rapidity distributions and angular variables describing the decay products are reweighted to NNLO calculations. Angular variables are validated with $Z$ data including the larger 8 TeV sample from 2012.

Separate fits are performed according to lepton charge, lepton flavour ($e$ or $\mu$) and to the $p_{\mathrm{T}}$ and $m_{\mathrm{T}}$ distributions. The fit results also provide a closure test of the quality of modelling.

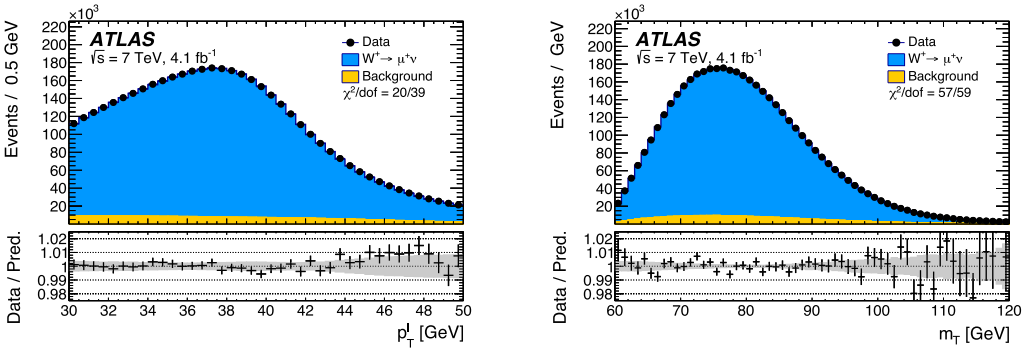


**Figure 7.** $W^{\pm}$ mass example fits to the $\mu^+$ $p_{\mathrm{T}}$ (left) and $m_{\mathrm{T}}$ (right) distributions.

**Table 1.** Systematic uncertainties in the $W^{\pm}$ mass measurements

| Uncertainty (MeV) | CDF (2.2 fb$^{-1}$) | D0 (4.3 fb$^{-1}$) | ATLAS (4.6 fb$^{-1}$) |
|---|---|---|---|
| Statistical | 12 | 13 | 7 |
| Experimental syst | 10 | 18 | 11 |
| QCD | n/a | n/a | 8 |
| PDF | 10 | 11 | 9 |
| QED | 4 | 7 | 6 |
| $p_{\mathrm{T}}(W)$ | 5 | 2 | n/a |

Two examples are shown in Figure 7. The final result is a weighted average, yielding $m_W = 80370 \pm 7(\mathrm{stat}) \pm 11(\mathrm{exp.\ syst.}) \pm 14(\mathrm{model})$ MeV, i.e. a combined precision of 19 MeV, equal to the CDF precision. The Particle Data Group [18] have made a new world average assuming 7 MeV common PDF uncertainty between the Tevatron and LHC results, as also shown in Figure 6.

The $W^{\pm}$ mass uncertainties are compared in Table 1, where the ATLAS uncertainties are taken from Table 11 of Ref. [19] for the combined result. To achieve a 10 MeV total uncertainty, the dominant PDF uncertainties will have to be reduced to about 5 MeV for the Tevatron results. With the huge samples of $W^{\pm}$ and $Z^0$ events at the LHC, there is scope to further reduce the experimental systematic uncertainties, and combining measurements with improved calculations to control the other modelling uncertainties.

### 4.2. *Weak mixing angle*

The forward-backward asymmetry of $Z^0 \to \ell\ell$ decays at hadron colliders depends on the mixture of up- and down-type quarks, and therefore depends strongly on the proton PDFs in deriving a measurement of $\sin^2\theta^{\mathrm{lept}}_{\mathrm{eff}}$.

The combined Tevatron measurements of $\sin^2\theta^{\mathrm{lept}}_{\mathrm{eff}}$ achieve a precision of 0.00033, as shown in Figure 8. There are now also competitive results from CMS [20] using 8 TeV data and a preliminary measurement from ATLAS [21] using 7 TeV data. The CMS measurement derives $\sin^2\theta^{\mathrm{lept}}_{\mathrm{eff}}$ from template fits to the forward backward asymmetry in different rapidity regions. The ATLAS measurement is a fit to the full angular description of the differential cross-section $pp \to Z \to \ell\ell$. It includes central $\mu\mu$ and $ee$ events, and an additional category of central-forward $ee$ events which bring extra precision, since the asymmetry is larger in the forward region. Now that these measurements approach the precision of the LEP and SLD experiments, particular care

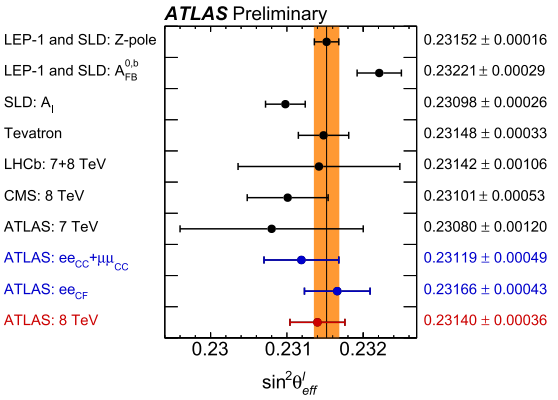


**Figure 8.** the most recent combinations of $\sin^2\theta^{\text{lept}}_{\text{eff}}$ measurements from LEP, SLD, the Tevatron and the LHC.

will be needed to be sure that consistent definitions of $\sin^2\theta^{\text{lept}}_{\text{eff}}$ are used, including QED and QCD corrections.

## 5. Future precision measurements

Several future $e^+e^-$ colliders are being discussed as worldwide projects that could contribute significantly to the precision measurements of the $Z^0$ and $W^\pm$ boson properties: the International Linear Collider (ILC) [22] which may be built in Japan, FCC-ee [23] a future circular collider proposed to be built at CERN and CEPC [24] a similar proposal to be built in China. Circular colliders will have several advantages: the most obvious one is extremely high statistics ($5\times10^{12}$ $Z^0$, $10^8$ $W^\pm$ $W^\pm$) compared with the GigaZ scenario where the ILC would collect up to three orders of magnitude less statistics. However, probably even more important is the ability of the circular collider proposals (FCC-ee and CEPC) to determine with high precision (better than 100 keV!) the centre-of-mass energies at the $Z^0$ pole and $W^\pm W^\pm$ threshold, thanks to the availability of transverse polarisation and resonant depolarisation (see previous sections). In addition, the FCC-ee proposal includes an optimised run plan to allow a complete programme of ancillary measurements of input parameters that currently would limit the precision of EW tests, a crucial example being the direct measurement [25] of $\alpha(m_Z{}^2)$ from the $Z^0-\gamma$ interference in the process $e^+e^-\to\mu^+\mu^-$.

The ILC ability to have longitudinal polarised beams (up to 80%) in the GigaZ option could allow for a measurement of the left-right asymmetry at the level of $\Delta(A_{LR})\sim10^{-4}$ [26] (two orders of magnitude better than existing measurements) and competitive with what equivalent measurements of the $\tau$ forward-backward polarisation asymmetry could provide at the FCC-ee (or CEPC), both sets of measurements measuring the same combination of couplings.

It is clear, however, that the best ultimate precision in most of the relevant observables for precision measurements of the $Z^0$ and $W^\pm$ bosons would come from the future circular colliders proposals. As an example, Table 2 shows the expected sensitivities for some of the relevant observables expected from the ILC-GigaZ proposal and FCC-ee. The quoted uncertainties include the current estimation of the systematic uncertainties, which for many of the observables quoted in Table 2 dominate the total uncertainty.

## 6. Conclusions

The four LEP experiments, ALEPH, DELPHI, L3 and OPAL, and the SLD experiment at the SLC, took precision measurements of $W^\pm$ and $Z^0$ boson properties to an unprecedented level after

**Table 2.** Measurement of selected EW quantities at the FCC-ee compared with present precision and ILC-GigaZ precision taken from references [26,27]

| Observable | Present value | ILC-GigaZ uncertainty | FCC-ee uncertainty |
|---|---|---|---|
| $m_Z$ (MeV) | 91186.7 ± 2.2 | 2.1 | 0.1 |
| $\Gamma_Z$ (MeV) | 2495.2 ± 2.3 | 1.0 | 0.1 |
| $R_\ell$ ($\times 10^3$) | 20767 ± 25 | 4 | 0.2–1.0 |
| $R_b$ ($\times 10^4$) | 2162.9 ± 6.6 | 1.2 | ~0.6 |
| $\sin^2\theta^{\rm lept}_{\rm eff}$ ($\times 10^5$) | 23148.0 ± 16 | 1.3 | 0.5 |
| $A_{\rm LR}$ ($\times 10^3$) | 151.3 ± 2.1 | 0.1 | - |
| $A^{{\rm FB},\tau}_{\rm pol}$ ($\times 10^3$) | 149.8 ± 4.9 | - | ~0.2 |
| $m_W$ (MeV) | 80350 ± 15 | 5 | 0.5 |

their first observation at UA1 and UA2. There was very close collaboration with accelerator experts to ensure that the LEP beam energy and SLC beam polarisation were well understood. The LEP electroweak working group and SLD heavy-flavour group ensured that the measurements were combined taking into account statistical correlations and systematic uncertainties. This pioneering inter-experiment cooperation expanded to other areas, including flavour physics and searches, so that the experiments could provide robust combined results taking into account all the "inside" information. Experiments at hadron colliders, with much larger samples of $W^\pm$ and $Z^0$ events, for improve the precision, in particular of the $W^\pm$-boson mass in leptonic final states. There are exciting prospects for future machines, which will probe $W^\pm$ and $Z^0$ physics improving the sensitivity to physics beyond the Standard Model in the decades to come.

## References


[1] E. Fermi, "Attempt at a theory of β-rays", *Il Nuovo Cimento* **11** (1934), p. 1.
[2] E. Fermi, "Attempt at a theory of β-rays. 1.", *Z. Phys.* **88** (1934), p. 161-177.
[3] S. L. Glashow, "Partial-symmetries of weak interactions", *Nuclear Phys.* **22** (1961), p. 579-588.
[4] S. Weinberg, "A model of leptons", *Phys. Rev. Lett.* **19** (1967), p. 1264-1266.
[5] A. Salam, *Proc. 8th Nobel Symp.*, 1968, 367 pages.
[6] F. J. Hasert *et al.*, "Search for elastic $\nu_\mu$ electron scattering", *Phys. Lett. B* **46** (1973), p. 121-124, [5.11(1973)].
[7] F. J. Hasert *et al.*, "Observation of neutrino like interactions without muon or electron in the Gargamelle neutrino experiment", *Phys. Lett. B* **46** (1973), p. 138-140, [5.15(1973)].
[8] C. Rubbia, P. McIntyre, D. Cline, *Producing Massive Neutral Intermediate Vector Bosons with Existing Accelerators*, Vieweg+Teubner Verlag, Wiesbaden, 1977, 683-687 pages.
[9] G. Arnison *et al.*, "Experimental observation of isolated large transverse energy electrons with associated missing energy at $s$ = 540 Gev", *Phys. Lett. B* **122** (1983), no. 1, p. 103-116.
[10] M. Banner *et al.*, "Observation of single isolated electrons of high transverse momentum in events with missing transverse energy at the cern pp collider", *Phys. Lett. B* **122** (1983), no. 5, p. 476-485.
[11] G. Arnison *et al.*, "Experimental observation of lepton pairs of invariant mass around 95-GeV/c**2 at the CERN SPS collider", *Phys. Lett. B* **126** (1983), p. 398-410, [7.55(1983)].
[12] P. Bagnaia *et al.*, "Evidence for $Z^0 \to e^+ e^-$ at the CERN anti-p p collider", *Phys. Lett. B* **129** (1983), p. 130-140, [7.69(1983)].
[13] R. Assmann *et al.*, "Calibration of center-of-mass energies at LEP-1 for precise measurements of Z properties", *Eur. Phys. J. C* **6** (1999), p. 187-223.
[14] R. Assmann *et al.*, "Calibration of centre-of-mass energies at LEP 2 for a precise measurement of the W boson mass", *Eur. Phys. J. C* **39** (2005), p. 253-292.
[15] "Precision electroweak measurements on the Z resonance", *Phys. Rep.* **427** (2006), no. 5-6, p. 257-454.
[16] "Electroweak measurements in electron-positron collisions at W-Boson-pair energies at LEP", *Phys. Rep.* **532** (2013), no. 4, p. 119-244.
[17] T. A. Aaltonen *et al.*, "Combination of CDF and D0 $W$-Boson mass measurements", *Phys. Rev. D* **88** (2013), no. 5, article ID 052018.

[18] M. Tanabashi *et al.*, "Review of particle physics", *Phys. Rev. D* **98** (2018), article ID 030001.
[19] "Measurement of the $W$-boson mass in pp collisions at $\sqrt{s}$ = 7 TeV with the ATLAS detector", *Eur. Phys. J. C* **78** (2018), no. 2, article ID 110, [Erratum: *Eur. Phys. J.* C78 (2018) no. 11, 898].
[20] "Measurement of the weak mixing angle using the forward-backward asymmetry of Drell-Yan events in pp collisions at 8 TeV", *Eur. Phys. J. C* **78** (2018), no. 9, article ID 701.
[21] ATLAS Collaboration, "Measurement of the effective leptonic weak mixing angle using electron and muon pairs from $Z$-boson decay in the ATLAS experiment at $\sqrt{s}$ = 8 TeV". Technical Report ATLAS-CONF-2018-037, CERN, Geneva, Jul 2018.
[22] H. Baer *et al.*, "The international linear collider technical design report - volume 2: Physics", 2013, preprint, https://arxiv.org/abs/1306.6352.
[23] A. Abada *et al.*, "Fcc-ee: the lepton collider", *Eur. Phys. J. Spec. Topics* **228** (2019), no. 2, p. 261-623.
[24] The CEPC Study Group, "CEPC conceptual design report: volume 1 - accelerator", 2018, preprint, https://arxiv.org/abs/1809.00285.
[25] P. Janot, "Direct measurement of $\alpha_{\mathrm{qed}}(mz^2)$ at the fcc-ee", *J. High Energy Phys.* **2016** (2016), no. 2.
[26] A. Irles, R. Pöschl, F. Richard, H. Yamamoto, "Complementarity between ILC250 and ILC-GigaZ", 2019, preprint, https://arxiv.org/abs/1905.00220.
[27] A. Abada *et al.*, "Fcc physics opportunities", *Eur. Phys. J. C* **79** (2019), no. 6, article ID 474.